

Electron Interference Effects on the Conductance of Doped Carbon Nanotubes

Alain Rochefort[†] and Phaedon Avouris^y

Centre de recherche en calcul appliqué (CERCA), Groupe Nanostructures et Biomateriaux,
5160 Boul. Decarie, bureau 400, Montréal, (Québec) Canada H3X 2H9.

^y IBM Research Division, T.J. Watson Research Center, P.O. Box 218, Yorktown Heights, NY
10598, USA.

(March 22, 2024)

Abstract

We investigate the effects of impurity scattering on the conductance of metallic carbon nanotubes as a function of the relative separation of the impurities. First we compute the conductance of a clean (6,6) tube, and the effect of model gold contacts on this conductance. Then, we compute the effect of introducing a single, two, and three oxygen atom impurities. We find that the conductance of a single-oxygen-doped (6,6) nanotube decreases by about 30% with respect to that of the perfect nanotube. The presence of a second doping atom induces strong changes of the conductance which, however, depend very strongly on the relative position of the two oxygen atoms. We observe regular oscillations of the conductance that repeat over an $0 \rightarrow 0$ distance that corresponds to an integral number of half Fermi wavelengths ($m_F = 2$). These fluctuations reflect strong electron interference phenomena produced by electron scattering from the oxygen defects whose contribution to the resistance of the tube cannot be obtained by simply summing up their individual contributions.

I. INTRODUCTION

Carbon nanotubes (CNTs) have very interesting electrical properties. Depending on their diameter and helicity it was predicted that they can be semiconductors or metals [1,2], and this was confirmed by scanning tunneling spectroscopy [3,4]. They can also sustain large current densities [5], and their electrical properties can be modified by doping [6]. These unique electrical characteristics coupled with their high mechanical stability and excellent thermal conductivity make the CNTs ideal candidates for use in nanoelectronics. Several possible applications such as their use as channels in field-effect transistors [7,8], single electron transistors [9], and diodes [10,11] have already been successfully demonstrated. It is therefore very important that a detailed understanding of electrical transport and energy dissipation in CNTs be developed. In addition to the quantized resistance due to the mismatch of the number of transmission channels in the tube and the metal contacts [12], additional sources of resistance are provided by the formation of Schottky barriers at the contacts [13,14], and by electron scattering from adsorbed or embedded impurity atoms and defects. A number of theoretical studies have appeared on this last issue. These studies have, so far, considered only scattering by individual defects [15-20], or, the contributions of a number of defects to the resistance of the tube were treated as being additive [21]. However, one important characteristic of transport in nanotubes is their long coherence lengths, especially at low temperatures. This coherence allows for interference effects involving scattering from the defect sites present in the probed nanotube segment.

Here we investigate two contributions to the resistance of nanotubes. First, we calculate the contact resistance arising from the imperfect coupling of nanotubes with model metal electrodes. Then we concentrate on the resistance produced by substitutional defects. We show that the relative position of defects can have a very important influence on the strength of scattering and on the resulting electrical resistance. Specifically, we calculate the attenuation of the transmission of a metallic nanotube induced by scattering from individual,

pairs, and triplets of oxygen defect sites as a function of their relative separation along the nanotube axis. Oxygen atoms are used here as model defects, but are likely to be introduced in nanotubes by oxidative purification of the nanotubes [22,23] or sonication.

II. COMPUTATIONAL DETAILS

The nanotube model used in the computations contains 948 carbon atoms (96 Å long) forming an arm chair (6,6) nanotube. The bond distance between carbon atoms of the NT is fixed to that in graphite 1.42 Å. This tube is bonded with its two dangling bond bearing ends to two metal electrodes [24]. Each electrode is modeled by a layer of 22 gold atoms in a (111) crystalline arrangement. The electrical transport properties of a system can be described in terms of the retarded Green's function [12,25]. The transmission function is computed by using the Landauer-Buttiker formalism as described in detail in ref. 12, and the effects of the semi-infinite electrodes are described by self-energies. The Green's function G_{NT} can be written in the form of block matrices separating explicitly the molecular Hamiltonian:

$$G_{NT} = [E S_{NT} - H_{NT} - \Sigma_1 - \Sigma_2]^{-1} \quad (1)$$

where S_{NT} and H_{NT} are the overlap and the Hamiltonian matrices, respectively, and $\Sigma_{1/2}$ are self-energy terms that describe the effect of the electrodes. They have the form $\Sigma_i = g_i g_i^\dagger$ with g_i the Green's function for the isolated semi-infinite electrodes [26,27], and \tilde{t}_i is a matrix describing the interaction between the NT and the Gold electrodes. The Hamiltonian and overlap matrices were determined using the extended Hückel method (EHM) [28] for the system: Gold-CNT-Gold. It has been shown that EHM gives results similar to those obtained on extended NTs with more sophisticated methods [29].

The transmission function, $T(E)$, that is obtained from this Green's function is given by [12]:

$$T(E) = T_{21} = \text{Tr}[G_{NT} G_{NT}^Y]: \quad (2)$$

In this formula, the matrices have the form :

$$G_{1,2} = i(\Gamma_{1,2} - \frac{Y}{1,2}): \quad (3)$$

The summation over all conduction channels in the molecule allows the evaluation of the conductance ($G(E_F)$) at the Fermi energy, i.e. for zero bias between the electrodes, $G(E_F) = (2e^2 T(E_F)) = h$.

Some of the configurations investigated in our oxygen-doping study are shown at top of Figure 1 (top). The first oxygen atom (dark atom in Fig. 1) is located near the middle of the tube between the electrodes while the position of the second oxygen atom is defined by the spacing number, i.e. the number of carbon atoms that are separating the two oxygen defect atoms along the zig-zag line. The distance between two adjacent circular carbon planes is 1.23 Å.

III. RESULTS AND DISCUSSION

Figure 1 (bottom) shows the variation of conductance ($G(E_F)$), in units of $2e^2 = h$, for the structurally perfect and oxygen-doped (6,6) nanotubes. The conductance of the perfect tube connected to the two model Au pads is calculated to be $2.3e^2 = h$, i.e. about 40% smaller than the expected $4e^2 = h$ value for a perfect CNT with ideal contacts. [15,30] This result shows that a sizable in series resistance can be introduced by non-ideal contacts. It is clear that contribution to the resistance of CNTs can obscure their intrinsic resistance quantization [24]. Depending on the nature of the interface, contact resistances can have contributions from many sources of non-ideality such as Schottky barriers or surface roughness. The value of the computed contact resistance ($\sim 5 k\Omega$) in our configuration compares well with contact resistances that can be inferred from experiments involving CNTs end-bonded to metal

electrodes [31].

Substitution of a carbon atom by an oxygen atom further reduces the conductance to about $1.6e^2/h$, a 30% decrease. For comparison, this reduction is similar than that produced by the introduction of a single vacancy which leads to $G(E_F) = 1.6e^2/h$. A 50% reduction in G was calculated using a somewhat different technique for a vacancy in a (4,4) nanotube. [15] More recently, a decrease of approximately 20% of the conductance at E_F was found on a (10,10) tube containing a vacancy with a more sophisticated technique [32]. We note that the reduction of the conductance of an $(n;n)$ tube introduced by a weak scatterer decreases with increasing n [15,18].

Introduction of a second doping oxygen atom changes the conductance. Most importantly, the magnitude of the change is not constant but is strongly correlated with the relative position of the second oxygen atom along the nanotube length. In fact, as Figure 1 shows, there is a strong oscillatory dependence of the conductance on the separation between the two O atoms. The values of the conductance $G(E_F)$ at the maxima are higher than the conductance of the CNT with a single O defect, and increase gradually as the O-O distance increases. The separation between two successive maxima (or minima) of $G(E_F)$ is equal to the width of three circular sections of the nanotube, i.e. $3 \times 1.23 \text{ \AA} = 3.69 \text{ \AA}$. The origin of the oscillatory behavior of $G(E_F)$ becomes clear by considering the electronic structure of the arm chair carbon nanotube. Figure 2 shows the highest occupied (HOMO) and lowest unoccupied (LUMO) molecular orbitals of the (6,6) model tube. In an arm chair nanotube these orbitals cross the Fermi level at the K-point [1,33], i.e. when $k = k_F = 2\pi/3a$, where $a = \frac{p}{3} R_{CC} = 2.46 \text{ \AA}$. Thus, the Fermi wavelength is $\lambda_F = 3a = 7.4 \text{ \AA}$ (see Fig. 2). We now see that the spacing between successive maxima (minima) of $G(E_F)$ corresponds to half a Fermi wavelength of the perfect nanotube.

In contrast to the strong dependence of G on the O-O separation, we find only a weak

dependence on the angle between the two O atoms. A calculation of G in which the O-O separation was set at $8 \approx k_F$ (29.5 Å), and where one O atom remained fixed while the second O atom was moved around a circular carbon section gave only a weak oscillation of $G(E_F)$ between the values of 1.87 and 1.91 e^2/h . This invariance to a C_6 (≈ 3) rotation can be understood by considering the frontier orbitals in Fig. 2 from which we see that such a symmetry operation leaves the wave function unchanged.

The effect of O atom substitution on the electronic structure of the CNT can be seen in Figure 3 which shows wave function contours of nanotube circular sections for the perfect tube (3A) and for the tube with two O atoms separated by 5 carbon ring sections, i.e. by 7.4 Å (3B). It can be seen that the effect of oxygen substitution is quite localized in the vicinity of the oxygen atoms. Further removed regions (not presented) show very similar wave function contours for both pure and doped CNTs. The main effect of O-doping is the generation of positive charges largely localized on the adjacent C atoms. We can then consider the two O atoms as forming a quasi-1D potential well with a length defined by the O-O atom separation that can scatter the Fermi level electrons. The transmission function T of such a system can then be written as [34]: $T = [1 + A \sin^2(k^0 d)]^{-1}$, where A depends on the ratio of the wavevectors of the incident wave (k) and of the wave inside the potential well (k^0). Transmission maxima will occur when $k^0 d = m\pi$, and minima when $k^0 d = (2m - 1)\pi/2$ (where $m = 1, 2, 3, \dots$). Thus, $G(E_F)$ will vary as a $\cos^2(k^0 d)$ with varying O-O atom separation d . The $\cos^2(k^0 d)$ envelope is shown by the dot-dashed line in Figure 1 (we have assumed that $k = k^0 = k_F$).

It is clear that the simple model involving electron interference of Fermi level electrons scattered by the potential well formed by the two O atoms can qualitatively explain the main features of Figure 1. However, deviations from this simple picture are also evident, and are most significant when the two O atoms are close to each other. First, in the 1-D potential well model, impurities separated by a distance of $m_F \approx 2$ should become transparent to the

incident electron waves, i.e. $T = 1$ [34], but although the transmission is indeed maximized at these separations, it never reaches unity. By comparing the effect of one O atom with the effects of two O atoms on G , and from the orbital contours of Fig. 3, we can conclude that O doping affects the conductance in two ways. Introduction of the first O atom into the CNT introduces a change in the local electronic structure which decreases the conductance of the tube. The introduction of the second O atom which reduces the symmetry to $C1$ leads to complex changes in the conductance of the tube. These changes depend on the relative distance between the two O atoms. The resulting contribution to the resistance due to the change in electronic structure is large, particularly when the two O atoms are close together, indicating a cooperative distortion of the electronic structure. At larger O-O separations, backscattering from the well becomes more important and G shows a clear O-O separation dependence as a result of interference between incident and back-reflected electrons in the well.

The interference effects observed with the two oxygen atom models can be generalized to CNTs doped with larger numbers of dopant atoms. The three oxygen atom case is particularly interesting. Some results are shown in Fig. 1 (open circles) where we have fixed the spacing between the two first oxygen atoms (O (1) and O (2)) to correspond to a constructive interference resonance ($4\pi = k_F$), and varied the position of the third O atom (O (3)). Again, oscillations in $G(E_F)$ are observed with maxima at O (2)-O (3) separations equal to $m\pi = k_F$, and minima when this distance is $(2m - 1)\pi = 2k_F$. The values of $G(E_F)$ computed for the three O atoms case are within the range found for the two O atoms case (Fig. 1). However, the same resonance is not observed when the outer two O atoms, O (1) and O (3) are kept at a distance corresponding to constructive interference, e.g. at $8\pi = k_F$, and O (2) is placed between them at a distance corresponding to destructive interference, e.g. at $7\pi = 2k_F$ from O (1). The O (2) atom causes a strong damping of the resonance leading to a $G(E_F)$ of only $0.98e^2/h$.

Next we consider the relation between $G(E_F)$ and the density of states at the Fermi energy, $DOS(E_F)$. The Drude conductivity of solids is proportional to the density of states, and a similar correlation was found by first-principles calculations on molecular wires [35]. As Fig. 4 shows, introduction of oxygen atoms in the arm chair nanotube increases the $DOS(E_F)$. However, Fig. 4 also shows that there is an anticorrelation between $G(E_F)$ and $DOS(E_F)$, the latter exhibiting approximately a $\sin^2(k_F d)$ dependence while the former shows a $\cos^2(k_F d)$ dependence. In Fig. 5 we also show the computed local density of states (LDOS) for nanotubes containing no oxygen atom (A), one oxygen atom (B), and two oxygen atoms located at distances leading to constructive (C) and destructive interference (D), respectively. These LDOS values represent the sum of the contributions to the density of states of the first three C atoms adjacent to the O impurity and of the impurity itself (full line). The contribution of the O atom alone is represented by the dashed-dotted line. The clean nanotube LDOS (5A) shows the first two van Hove singularities on either side of E_F . Upon introduction of the first O atom a new quasi-bound state is formed centered at about 0.3 eV above E_F with a tail that extends to E_F (5B). This state is quite similar to that produced by the introduction of nitrogen [32]. Position dependent modifications of the electronic structure with respect to Fermi energy are observed upon introduction of the second O atom (5C and 5D).

The behavior of $DOS(E_F)$ in Fig. 4 can be understood by considering the changes in bonding produced by the substitution of a C atom by an O atom. This substitution generates non-bonding states whose center of gravity is near E_F . Thus, although there is an increase in $DOS(E_F)$, the conductance does not increase because of the localized nature of these O-induced states. This leads to an anti-correlation between $DOS(E_F)$ and $G(E_F)$. Turning to the behavior of the LDOS (Fig. 5), we note that there is a minimum at the O site when the O-O separation corresponds to a resonance ($l = k_F$). This is likely due to the formation of the nodal front of the standing wave between the O (1) and O (2) atoms (Fig. 5C). The LDOS in Fig. 5D where the O-O separation ($l = 2k_F$) leads to destructive

interference, shows no such minimum.

IV . C O N C L U S I O N S

In conclusion, we have shown that interference effects involving scattering from pairs of defects in carbon nanotubes and defect-defect interactions can have a strong influence on the electrical resistance of the tubes. Due to the long coherence lengths in carbon nanotubes, the net contribution of a number of scatterers cannot be determined merely by the sum up of their individual contributions.

V . A C K N O W L E D G M E N T

We thank Francois Leonard and Massimiliano Di Ventura for their helpful comments on the manuscript.

REFERENCES

- [1] Saito, R .; Fujita, M .; Dresselhaus, G .; Dresselhaus, M .S. Appl. Phys. Lett. 1992, 60, 2204.
- [2] McIntire, J.W .; Dunlap, B .I.; White, C .T. Phys. Rev. Lett. 1992, 68, 631.
- [3] Wildoer, J.W .G .; Venema, L .C .; Rinzler, A .G .; Smalley, R .E .; Dekker, C . Nature (London) 1998, 391, 59.
- [4] Odom, T .W .; Huang, J.-L .; Kim, P .; Lieber, C .M .; Nature (London) 1998, 391, 62.
- [5] Aouris, Ph.; Martel, R .; Ikeda, H .; Hersam, M .; Shea, H .R .; Rochefort, A . Science and Applications of Nanotubes, Tománek D ., Enbody, R .J., Eds.; Kluwer Academic/Plenum Publishers: New York, 2000.
- [6] Lee, R .S .; Kim, H .J .; Fisher, J .E .; Thess, A .; Smalley, R .E .; Nature (London) 1997, 388, 255.
- [7] Tans, S .J .; Verschueren, A .R .M .; Dekker, C . Nature (London) 1998, 393, 49.
- [8] Martel, R .; Schmidt, T .; Shea, H .R .; Hertel, T .; Aouris, Ph. Appl. Phys. Lett. 1998, 73, 2447.
- [9] Bockrath, M .; Cobden, D .H .; McEuen, P .L .; Chopra, N .G .; Zettl, A .; Thess, A .; Smalley, R .E . Science 1997, 275, 1922.
- [10] Collins, P .G .; Zettl, A .; Bando, H .; Thess, A .; Smalley, R .E .; Science 1997, 278, 5335.
- [11] Yao, Z .; Postma, H .W .Ch.; Balents, L .; Dekker, C . Nature (London) 1999, 402, 273.
- [12] Datta, S. Electronic Transport in Mesoscopic Systems, Cambridge University Press: Cambridge, U K ., 1995.
- [13] Leonard, F .; Terso, J. Phys. Rev. Lett. 1999, 83, 5174.
- [14] Xue, Y .; Datta, S. Phys. Rev. Lett. 1999, 83, 4844.

- [15] Chico, L.; Benedict, L X.; Louie, S G.; Cohen, M L. Phys. Rev. B 1996, 54, 2600.
- [16] Lambin, Ph.; Vigneron, J P.; Lucas, A A. Synthetic Metals 1996, 77, 249.
- [17] Crespi, V H.; Cohen, M L.; Rubio, A. Phys. Rev. Lett. 1997, 79, 2093.
- [18] White, C T.; Todorov, T N. Nature (London) 1998, 393, 240.
- [19] Ando, T.; Nakanishi, T.; Saito, R. J. Phys. Soc. Jpn. 1998, 67, 2857.
- [20] Anantram, M P.; Govindan, T R. Phys. Rev. B 1998, 58, 4882.
- [21] Kostyrko, T.; Bartkowiak, M.; Mahan, G D. Phys. Rev. B 1999, 60, 10735; Phys. Rev. B 1999, 59, 3241.
- [22] He, H.; Klinowski, J.; Foster, M.; Lerf, A. Chem. Phys. Lett. 1998, 287, 53.
- [23] Kuznetsova, A.; Jates, J.T. Jr.; Liu, J.; Smalley, R E. J. Chem. Phys. 2000, 112, 9590.
- [24] Rochefort, A.; Aouris, Ph.; Lesage, F.; Salahub, D R. Phys. Rev. B 1999, 60, 13824.
- [25] Economou, E N. Green's Functions in Quantum Physics, Springer-Verlag: New York, 1983.
- [26] Tian, W.; Datta, S.; Hong, S.; Reifenberger, R.; Henderson, J.I.; Kubiak, C P. J. Chem. Phys. 1998, 109, 2874.
- [27] Papaconstantopoulos, D A. Handbook of the Band Structure of Elemental Solids, Plenum Press: New York, 1986.
- [28] Landrum, G. YAEHMO P (Yet Another Extended Huckel Molecular Orbital Package), Cornell University, Ithaca, NY, 1995.
- [29] Rochefort, A.; Salahub, D R.; Aouris, Ph. J. Phys. Chem. 1999, 103, 641.
- [30] Frank, S.; Poncharal, P.; Wang, Z. L.; de Heer, W A. Science 1998, 280, 1744.
- [31] Dai, H.; Kong, J.; Zhou, C.; Franklin, N.; Tomblar, T.; Cassell, A.; Fan, S.; Chapline,

- M .J. Phys. Chem .B 1999, 103, 11246.
- [32] Choi, H .J.; Ihm , J.; Louie, S.G .; Cohen, M .L. Phys. Rev. Lett. 2000, 84, 2917.
- [33] Rubio, A .; Sanchez-Portal, D .; Artacho, E .; Ordejón, P .; Solé, J.M . Phys. Rev. Lett. 1999, 82, 3520.
- [34] Merzbacher, E . Quantum Mechanics, John Wiley & Sons: New York, 1970.
- [35] Lang, N.D .; Avouris, Ph. Phys. Rev. Lett. 1998, 81, 3515.; Phys. Rev. Lett. 2000, 84, 358.

FIGURES

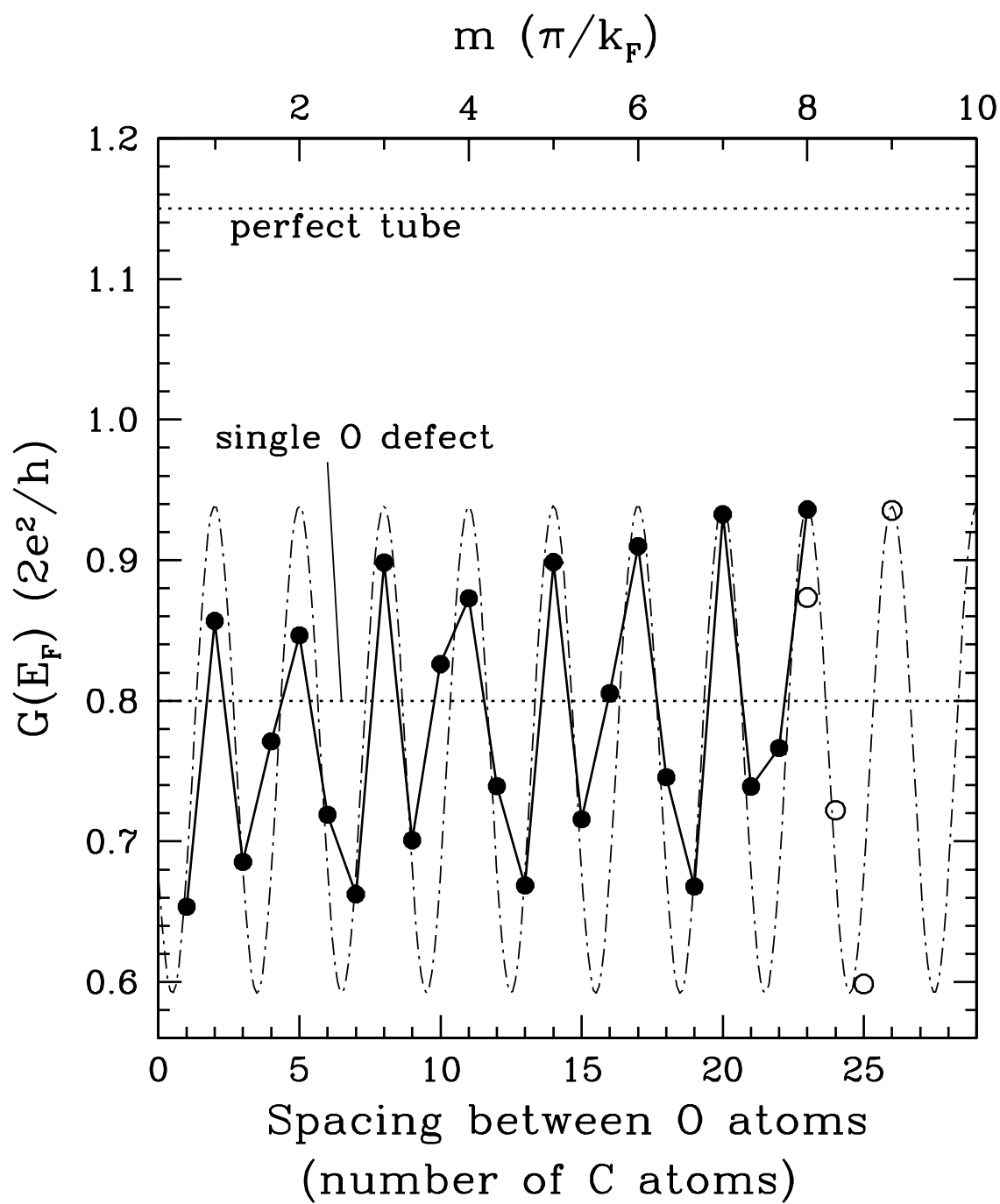
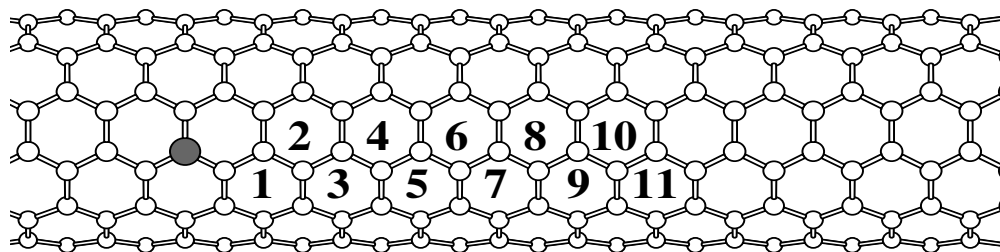
FIG .1. Top: Schematic showing the different positions of two oxygen atom dopants in the (6,6) carbon nanotube model. The position of the first atom (dark) is fixed, while the possible positions of the second O-atom are indicated by the numbers. Bottom : Computed conductance (in units of $2e^2/h$) of a (6,6) nanotube under different conditions. The dotted line indicates the conductance of the clean nanotube that includes a series resistance due to the imperfect contacts with gold pads (see text). The second dotted line shows the conductance after the incorporation of a single oxygen atom. The solid circles give the conductance of the tube after the incorporation of a second oxygen atom as a function of the separation between the two O-atoms. The empty circles give the conductance of the tube doped with three oxygen atoms when the distance between the first and the second O-atoms is fixed at $4a_0$ (14.8 Å) and the position of the third is varied.

FIG .2. Representation of: (A) the highest occupied molecular orbital (HOMO), and (B) the lowest unoccupied (LUMO) orbital of an undoped (6,6) arm chair nanotube model.

FIG .3. Comparison of the orbital contours of the highest occupied orbital (HOMO) of (A): a clean (6,6) tube, and (B): a tube doped by two oxygen atoms (dark circles). The contours are generated in a plane perpendicular to the nanotube axis.

FIG .4. Variation of the total density of states at the Fermi level DOS (E_F) of oxygen-doped nanotubes. The dot-dashed line shows a $\sin^2(k_F d)$ envelope

FIG .5. Local density of states (LDOS) in the vicinity of the oxygen impurities in a (6,6) carbon nanotube containing no oxygen atom (A), one oxygen atom (B), two O atoms located at a resonance position (C), and at an antiresonance position (D). Full lines represent the DOS contributions from the impurity itself and the first three neighboring carbon atoms, while dashed-dotted lines give the DOS of the impurity only. The O-O separation is given in panels C and D.



This figure "figure2.gif" is available in "gif" format from:

<http://arxiv.org/ps/cond-mat/0009335v1>

This figure "figure3.gif" is available in "gif" format from:

<http://arxiv.org/ps/cond-mat/0009335v1>

